

# Very Light Scalar Top Quarks at the LHC

Karol Krizka<sup>(a,b,c)</sup>, Abhishek Kumar<sup>(b)</sup>,  
David E. Morrissey<sup>(b)</sup>

(a) *Department of Physics, Simon Fraser University, Burnaby, BC  
V5A 1S6, Canada*

(b) *TRIUMF, 4004 Wesbrook Mall, Vancouver, BC V6T 2A3, Canada*

(c) *Enrico Fermi Institute and Department of Physics, University of  
Chicago, 5620 S. Ellis Avenue, Chicago, IL 60637, USA*

*email: kkrizka@uchicago.edu, abhishek@triumf.ca, dmorri@triumf.ca*

November 14, 2018

## Abstract

A very light scalar top (stop) superpartner is motivated by naturalness and electroweak baryogenesis. When the mass of the stop is less than the sum of the masses of the top quark and the lightest neutralino superpartner  $\chi_1^0$ , as well as the of the masses of the lightest chargino and the bottom quark, the dominant decay channels of the stop will be three-body (3B:  $bW^+\chi_1^0$ ), four-body (4B:  $bf\bar{f}'\chi_1^0$ ), or flavour violating (FV:  $c\chi_1^0$ ). In this work, we investigate the direct and indirect constraints on a light stop, we compute the relative decay branching fractions to these channels, and we study the sensitivity of existing LHC searches to each of them.

# 1 Introduction

Supersymmetry can protect the scale of electroweak symmetry breaking from destabilising quantum corrections provided the masses of the Standard Model (SM) superpartners are not too large [1]. The most important states in this regard are those that couple the most strongly to the Higgs fields, namely the scalar top quarks (stops). To give the desired protection, the two stop mass eigenstates should be considerably lighter than a TeV [2].

A light stop can also play an important role in cosmology. The baryon asymmetry can be created within the minimal supersymmetric standard model (MSSM) by the process of electroweak baryogenesis (EWBG) if at least one of the stops is lighter than the top quark [3, 4, 5]. A light stop can help to produce the observed dark matter relic density as well. When the lightest superpartner (LSP) is a mostly-Bino neutralino, the mechanism of thermal freeze-out tends to create too much dark matter. However, a light stop that is close in mass to the neutralino LSP can reduce its thermal abundance to the observed value by coannihilation [6, 7, 8, 9].

For these many reasons, an intense search for light stops is underway at the Large Hadron Collider (LHC), and a broad range of theoretical studies have been performed recently to find the most promising search channels [10, 11, 12, 13, 14, 15, 16, 17, 18, 19]. The two decay channels that have been studied in the most detail are

$$\tilde{t}_1 \rightarrow t\chi_1^0, \quad \tilde{t}_1 \rightarrow b\chi_1^+ \quad (2B) , \quad (1)$$

where  $\chi_1^0$  is the lightest neutralino and  $\chi_1^+$  is the lightest chargino. When the stop is too light to decay in these channels, the dominant decay modes can involve three- or four-body final states such as [20, 21, 22]

$$\tilde{t} \rightarrow b\chi_1^0 W^{(*)} \quad (3B, 4B) , \quad (2)$$

or have flavour violation [20, 21],

$$\tilde{t} \rightarrow c\chi_1^0 \quad (FV) . \quad (3)$$

Of these, the two-body FV mode has been studied the most extensively [23, 24, 25, 26, 27, 28, 29, 30, 31, 32, 33, 34, 35, 36, 37], and is typically assumed to be the exclusive decay channel when the three-body decay is kinematically forbidden.

In this work we study the LHC collider signals of a very light stop, with  $m_{\tilde{t}_1} \leq m_t + m_{\chi_1^0}$ , in a comprehensive way. We place an emphasis on the scenario where only the 4B and FV decay channels are open. The branching ratios of these modes depend on the underlying flavour structure of the theory, and we make the assumption that it is governed by Minimal Flavour Violation (MFV). In this case, we find that the 4B channel is frequently the dominant one despite its suppression by the large final-state phase space. To our knowledge, the LHC signals of a light stop decaying in this way have not been studied in detail.

The outline of this paper is as follows. We begin in Sec. 2 by presenting the relevant stop interactions and the corresponding mass matrix, as well as our assumptions about MFV flavour mixing. Next, in Sec. 3 we investigate the indirect limits on very light stops from precision electroweak and flavour measurements. With these bounds in hand, we study the dominant decay channels of the light stop in Sec. 4. We then apply these results to make estimates of the sensitivity of existing LHC searches to a light stop. Finally, Sec. 6 is reserved for our conclusions. Some technical details can be found in the Appendix A.

## 2 Stop Parameters

To begin, we define our parameters and specify our assumptions about the flavour structure of the theory. In the absence of flavour mixing, the tree-level stop mass matrix is [1]

$$\mathcal{M}_t^2 = \begin{pmatrix} m_{Q_3}^2 + (\frac{1}{2} - \frac{2}{3}s_W^2)c_{2\beta}m_Z^2 + m_t^2 & m_t X_t^* \\ m_t X_t & m_{U_3^c}^2 + \frac{2}{3}s_W^2 c_{2\beta}m_Z^2 + m_t^2 \end{pmatrix}, \quad (4)$$

with  $m_{Q_3}^2$  and  $m_{U_3^c}^2$  the scalar soft squared masses,  $m_t$  mass of the top quark,  $\tan \beta$  the ratio of Higgs vacuum expectation values (VEVs), and

$$X_t = A_t - \mu^* / \tan \beta \quad (5)$$

parametrizes the left-right (LR) stop mixing. A light stop mass eigenstate arises for small soft mass parameters or large LR mixing.

Flavour mixing within the Yukawa couplings of the SM translates into some degree of flavour mixing in its supersymmetric extension. Additional sources of flavour mixing can arise from soft supersymmetry breaking parameters, although these are strongly constrained by experiment [38, 39]. In

this work we will assume a specific flavour structure for the soft terms that is relatively consistent with existing flavour bounds, namely Minimal Flavour Violation (MFV) [40].

The structure of MFV is based on the observation that the SM has a global  $SU(3)^5$  flavour symmetry in the absence of Yukawa couplings. By promoting the Yukawas to spurions that transform under the global flavour group, the SM is made invariant under the symmetry. The flavour group is then broken only by the background values of the spurions. As applied to theories of new physics beyond the SM, MFV requires that this flavour structure continue to hold true, with any new sources of flavour mixing proportional to the Yukawa spurions.

For the MSSM, the MFV hypothesis restricts the flavour structure of the soft parameters. The soft scalar mass-squareds become  $6 \times 6$  matrices. To leading order in the Yukawa expansion they are given by [40, 41]

$$m_Q^2 = \tilde{m}^2(a_1\mathbb{I} + b_1Y_uY_u^\dagger + b_2Y_dY_d^\dagger + b_3Y_dY_d^\dagger Y_uY_u^\dagger + b_4Y_uY_u^\dagger Y_dY_d^\dagger) \quad (6)$$

$$m_{U^c}^2 = \tilde{m}^2(a_2\mathbb{I} + b_5Y_u^\dagger Y_u + c_1Y_u^\dagger Y_dY_d^\dagger Y_u) \quad (7)$$

$$m_{D^c}^2 = \tilde{m}^2(a_3\mathbb{I} + b_6Y_d^\dagger Y_d) . \quad (8)$$

Similarly, the squark trilinear couplings are

$$a_u = A(a_4\mathbf{1} + b_7Y_dY_d^\dagger)Y_u \quad (9)$$

$$a_d = A(a_5\mathbf{1} + b_8Y_uY_u^\dagger)Y_d . \quad (10)$$

The coefficients  $a_i$ ,  $b_i$ , and  $c_i$  parametrize the expansion and are expected to be on the order of unity or less. Their values may be restricted within specific theories of flavour, but we treat them as free parameters at the superpartner mass scale.<sup>1</sup> See Appendix A for a more complete description of our conventions for flavour and the soft masses.

To compute flavour-violating stop decays, it is convenient to choose a specific basis for the Yukawa matrices where the up-Yukawas are diagonal,

$$Y_u = \lambda_u \quad Y_d = V\lambda_d , \quad (11)$$

where  $V$  is the CKM matrix, and  $\lambda_{u,d}$  are the diagonal up- and down-Yukawa matrices.

---

<sup>1</sup>This is consistent with but more general than the commonly-used assumption that the flavour mixing vanishes at some high-energy scale.

For our study we choose a set of fiducial soft parameters that allows us to isolate a light stop state. We take  $\tilde{m} = 1500$  GeV and  $a_1 = a_2 = a_3 = 1$ , which has the effect of decoupling the first- and second-generation squarks, and we choose similar soft masses for the sleptons. Much smaller values of  $(m_Q^2)_{33}$  and  $(m_{U^c}^2)_{33}$  are obtained by suitable choices of  $b_1$  and  $b_5$ , and these translate into one or more light squark states. Since these states only contain very small admixtures of the first- and second-generation squarks, we identify them with a pair of stops and a (mainly left-handed) sbottom. The rest of the  $b_i$  and  $c_i$  parameters are scanned over the range  $[-1, 1]$ . We also set the gluino soft mass to  $M_3 = 1000$  GeV, but we consider a range of values for the electroweak gaugino soft masses  $M_1$  and  $M_2$  and the Higgsino mass  $\mu$ . In implementing these values within the spectrum generators SuSpect 2.41 [42] and SoftSUSY 3.3.5 [43], we input these parameters as running values defined at  $M_S = \sqrt{m_t m_Q}$ . Finally, we consider the specific representative cases of  $\tan \beta = 10, 30$ .

### 3 Limits on a Light Stop

Stops have been searched for extensively at the Tevatron and the LHC. A light stop can also influence a number of SM observables by its contributions in loops. We review here the existing limits on stops from direct collider searches and we study the indirect limits on a light stop from precision electroweak measurements and flavour violation. We also comment on the constraints imposed by the rates of Higgs production and decay.

#### 3.1 Direct Collider Searches

The ATLAS and CMS collaborations at the CERN LHC have succeeded in confirming the SM to such an extent that squarks of the first and second generations are constrained to be heavier than a TeV [44, 45]. More recently, these collaborations have turned their attention to investigating the squarks of the third generation created both directly and indirectly. Recent studies rule out direct stop pair production for stop masses up to nearly 600 GeV under the assumption that the only decay is  $\tilde{t} \rightarrow t\chi_1^0$  with  $m_{\chi_1^0} \rightarrow 0$  and  $\chi_1^0$  a stable LSP [46, 47]. The limits weaken for larger values of the LSP mass, but remain in the range of many hundreds of GeV. Searches for direct sbottom pair production with  $\tilde{b} \rightarrow b\chi_1^0$  yield similar bounds on the lightest

sbottom mass [48]. Related searches for direct stop production with the decay  $\tilde{t} \rightarrow b\chi_1^+$  together with  $\chi_1^+ \rightarrow W^{(*)}\chi_1^0$  also give exclusions as large as  $m_{\tilde{t}} > 450$  GeV [46, 47]. Finally, light stops or sbottoms can be created in gluino decays. Assuming one or the other of the topologies  $\tilde{g} \rightarrow t\bar{t}\chi_1^0$  with  $\tilde{t} \rightarrow t\chi_1^0$  or  $\tilde{g} \rightarrow b\bar{b}$  with  $\tilde{b} \rightarrow b\chi_1^0$ , the constraint on the gluino mass extends up to  $m_{\tilde{g}} = 1.3$  TeV [49, 50].

Collider limits on stops and sbottoms can be much weaker when they decay in other ways, such as the 3B, 4B, and FV channels. Searches at LEP rule out a stop decaying in the FV channel up to about 100 GeV [51], and we expect similar limits to hold for the 3B and 4B decays. At the Tevatron, specific searches for a light stop in the FV mode give limits up to  $m_{\tilde{t}} \simeq 180$  GeV, but these limits disappear when the stop becomes moderately degenerate with the LSP [52, 53]. Almost no limit is expected when the 3B or 4B channels are dominant [24]. The LHC collaborations have not performed dedicated searches for a stop in the 3B, 4B, and FV modes. The goal of this work is deduce the sensitivity of existing LHC searches to these stop channels.

### 3.2 Indirect Bounds from Electroweak and Flavour

The most important effect of a light stop on precision electroweak observables is to modify the prediction for the mass of the  $W$  boson, corresponding to a shift in  $\Delta\rho$  (or  $T$  in the  $STU$  parametrization of oblique parameters [54]). This effect has been studied recently in Refs. [55, 56, 57] in light of the improved determination of  $M_W$  [58] together with evidence for a Higgs boson of mass  $m_h = 125$  GeV [59, 60]. These results imply  $\Delta\rho = (4.2 \pm 2.7) \times 10^{-4}$  [56, 57].

The change in  $\Delta\rho$  due to light stops is given by [61]

$$\Delta\rho \simeq \frac{3G_F}{8\sqrt{2}\pi^2} \left[ -s_t^2 c_t^2 F_0(m_{t_1}^2, m_{t_2}^2) + c_t^2 F_0(m_{t_1}^2, m_{b_L}^2) + s_t^2 F_0(m_{t_2}^2, m_{b_L}^2) \right], \quad (12)$$

where  $\theta_{\tilde{t}}$  is the stop mixing angle and  $F_0(x, y)$  is a loop function,

$$F_0(x, y) = x + y - \frac{2xy}{x - y} \ln \left( \frac{x}{y} \right). \quad (13)$$

We apply this formula in the present case where we have squark flavour mixing dictated by the MFV paradigm. Since the inter-generational mixing

is numerically small, we are able to identify specific squark mass eigenstates with  $\tilde{t}_1$ ,  $\tilde{t}_2$ , and  $\tilde{b}_L$ , and apply this formula directly. Additional corrections due to flavour mixing are expected to be highly subleading. We also neglect the contributions from neutralinos and charginos, which are also expected to be less important [61, 62, 63].

A light stop can also contribute to flavour mixing, and to the branching fraction  $\text{BR}(B \rightarrow X_s \gamma)$  in particular. This effect is present even if the scalar soft parameters are all diagonal in the super-CKM basis (discussed in Appendix A) due to loops involving a top and a charged Higgs or a stop and a chargino. These new contributions vanish in the supersymmetric limit, but can modify the branching fraction when supersymmetry breaking is present [64, 65, 66]. In our analysis, we use the HFAG experimental result  $\text{BR}(B \rightarrow X_s \gamma) = (3.55 \pm 0.24 \pm 0.09) \times 10^{-4}$  [67] together with the SM prediction of  $\text{BR}(B \rightarrow X_s \gamma) = (3.15 \pm 0.23) \times 10^{-4}$  from Ref. [68]. We also consider limits from  $\text{BR}(B_s \rightarrow \mu^+ \mu^-)$  [69] and  $\Delta_0(B \rightarrow K^* \gamma)$  [39, 67].

We investigate the contributions of a light stop to  $\text{BR}(B \rightarrow X_s \gamma)$  and other flavour observables by using SoftSUSY 3.3.5 [43] to compute the superpartner mass spectrum and mixings and passing the output to SuperISO 3.3 [70] to evaluate the modifications to flavour observables. Input and output are achieved in the SLHA2 format [71], and a detailed description of the interface is given in Appendix A.

With these tools, we have performed a series of scans over stop parameters by varying the  $A$ ,  $b_i$ , and  $c_i$  MFV parameters, while holding fixed  $a_i = 1$  and  $\tilde{m}^2 = (1500 \text{ GeV})^2$  to maintain heavy first- and second-generation sfermions near 1500 GeV. We have also set  $M_3 = 1000 \text{ GeV}$ ,  $M_1 = 200 \text{ GeV}$ ,  $M_2 = 350 \text{ GeV}$ , and  $\mu = M_A = 500 \text{ GeV}$ . The resulting allowed regions, consistent with both precision electroweak and flavour constraints at the  $2\sigma$ -level,<sup>2</sup> are shown in Fig. 1 for different values of the stop mass  $m_{\tilde{t}_1}$ , the stop mixing angle  $|\cos \theta_{\tilde{t}}|$ ,<sup>3</sup> and the stop mass-matrix mixing parameter  $X_t = X_{t_{33}}$ . In both panels, we have fixed  $\tan \beta = 10$  and we have restricted  $100 \text{ GeV} < m_{\tilde{t}_1} < 300 \text{ GeV}$  and  $m_{\tilde{b}_1} > 100 \text{ GeV}$ . We also show the effects of imposing additional restrictions on the mass of the lightest sbottom:  $m_{\tilde{b}_1} = 300 \text{ GeV}$ ,  $600 \text{ GeV}$ , which are motivated by the strong limits placed on sbottoms by the recent analysis of Ref. [48].

Our primary conclusion from Fig. 1 is that electroweak and flavour bounds

---

<sup>2</sup>The ranges are  $\Delta\rho \in [-1.2, 9.4] \times 10^{-4}$  and  $\text{BR}(B \rightarrow X_s \gamma) \in [2.77, 4.33] \times 10^{-4}$ .

<sup>3</sup>Our convention is  $|c_{\tilde{t}}| = 1$  (0) when the lightest stop is purely left(right)-handed.

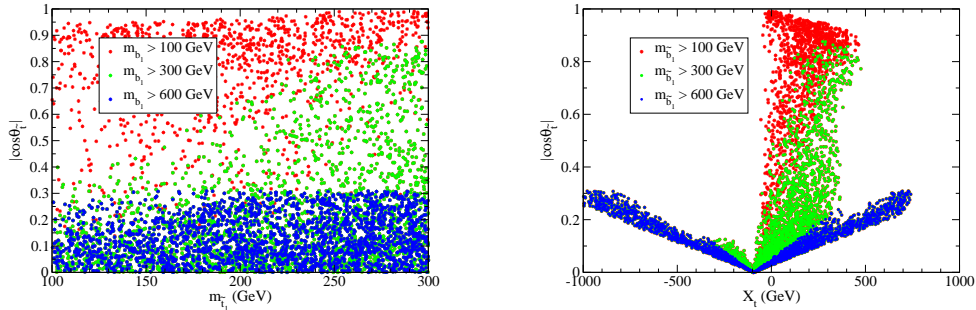


Figure 1: Allowed light stop mass and mixing angles for  $\tan \beta = 10$ .

alone permit a broad range of mixing angles for a light stop, but that demanding a heavier sbottom forces the light stop to be mainly right-handed.<sup>4</sup> Despite the broad range of allowed mixing angles, we also find a severe restriction on the stop mixing parameter  $X_t$  for smaller values of  $m_{Q_{33}}^2$ , which comes partly from  $\Delta\rho$  but mainly from  $\text{BR}(B \rightarrow X_s \gamma)$ . We have also examined the allowed ranges for  $\tan \beta = 30$ , and we obtain similar results, albeit with a stronger restriction on  $X_t$ . The limitations on  $X_t$  derive from an interplay between the chargino-stop and charged Higgs-top contributions to  $\text{BR}(B \rightarrow X_s \gamma)$ . These must cancel to some extent when there is a light stop in the spectrum, with the specific condition depending mainly on  $\mu$ ,  $M_A$ ,  $\tan \beta$ , and  $X_t$ . Even so, at the expense of some amount of tuning between these parameters, a broad range of stop properties is possible.

Let us also mention that among the bounds from flavour mixing, we find that  $\text{BR}(B \rightarrow X_s \gamma)$  gives the most significant limit for the parameters we studied, and is more restrictive than  $\text{BR}(B_s \rightarrow \mu^+ \mu^-)$  [69] and  $\Delta_0(B \rightarrow K^* \gamma)$  [67]. We also find that the contributions to flavour observables are typically dominated by the CKM mixing already present in the super-CKM basis. More precisely, the deviations from flavour-diagonal squark mass matrices in the super-CKM basis allowed by MFV do not appreciably change the effects of the superpartners on the flavour observables we have studied. Indeed, in the case of  $\text{BR}(B \rightarrow X_s \gamma)$ , we find substantial agreement with SuSpect 2.41 [42] which does not include any additional (non-super-CKM) flavour mixing.

<sup>4</sup> A light sbottom might still be consistent with LHC searches if it is highly degenerate with both the light stop and the neutralino LSP [48].

### 3.3 Higgs Production and Decay Rates

Light stops are also closely linked to the mass of the SM-like  $h^0$  Higgs boson in the MSSM. For many of the sets of stop masses we consider in this work, the mass of  $h^0$  lies well below the mass of the tentative Higgs resonance near 125 GeV [72, 73]. Within the MSSM, this discrepancy can be resolved by pushing the left-handed stop soft parameter  $m_{Q_{33}}^2$  to values well above the TeV scale [3, 74]. This problem can also be addressed by expanding the field content to include an additional singlet, as in the NMSSM. In both cases, these fixes can be achieved without necessarily altering the collider signatures of the light stop.

A light stop can also modify the production and decay rates of the  $h^0$  Higgs [75]. When the light state is mainly unmixed, the effect is to enhance the production rate in gluon fusion and to suppress the branching fraction to photon pairs [76, 77, 78]. Conversely, when the light stop is highly mixed it has the opposite effect, pushing down the rate for gluon fusion and increasing the branching ratio to diphotons [79]. The Higgs rates can also be modified by the presence of other MSSM (or beyond) superpartners that run in the loops [74, 80] or that mix with the Higgs [81, 82]. Again, these extensions of the MSSM need not modify the collider signals of the light stop.

Light stops can also contribute in a more direct way to Higgs searches by the formation of stoponium, a stop-antistop bound state [83, 84, 85, 86]. Stoponium decays can mimic those of a Higgs boson. However, for  $m_{\tilde{t}_1} > m_{h^0}$ , the dominant stoponium decay mode is frequently to a pair of  $h^0$  Higgs bosons (particularly if the stop state is not highly mixed). Current LHC searches do not appear to be sensitive to this decay channel [85].

For these various reasons, we do not constrain the spectrum of light stops based on searches for and the tentative discovery of the  $h^0$  Higgs boson. Instead, we focus on the direct LHC limits on a light stop state.

## 4 Light Stop Decay Modes

We consider the decays of a light stop to the lightest neutralino or chargino in the spectrum, taking the rest of the superpartners to be heavy. We also focus on the case where  $\tilde{t} \rightarrow t\chi_1^0$  is kinematically forbidden. The stops then have four possible decay modes:

1. two-body (2B):  $b\chi_1^+$ .

2. three-body (3B):  $bW^+\chi_1^0$ .
3. four-body (4B):  $bf\bar{f}'\chi_1^0$ .
4. flavour-violating (FV):  $c\chi_1^0$ .

Our analysis shows that each of these modes tends to dominate in a different kinematic region, depending on the stop-neutralino and stop-chargino mass differences.

#### 4.1 Flavour-Violating Stop Decays in MFV

The most model-dependent of these decays modes is the FV channel. We apply the results of Ref. [87] to calculate the FV decay width within the framework of Minimal Flavour Violation (MFV) [40]. The general form of the stop-charm-neutralino coupling is [87]

$$\mathcal{L}_{c\tilde{t}\tilde{\chi}_1^0} = \bar{c}(y_L P_R + y_R P_L)\tilde{\chi}_1^0 \tilde{t} + \text{h.c.} , \quad (14)$$

in terms of which the FV decay width is given by

$$\Gamma = \frac{Y^2}{16\pi} m_{\tilde{t}} \left( 1 - \frac{m_{\tilde{\chi}_1^0}^2}{m_{\tilde{t}}^2} \right)^2 , \quad (15)$$

where  $Y = \sqrt{|y_L|^2 + |y_R|^2}$ .

The couplings  $y_L$  and  $y_R$  can be computed reliably in the mass-insertion approximation. The relevant flavour mixings in this case arise from the following off-diagonal elements of the soft masses [87]:

$$\begin{aligned} (\tilde{m}_{Q_L}^2)_{23} &= \tilde{m}^2 b_2 (Y_d Y_d^\dagger)_{23} = \tilde{m}^2 b_2 \lambda_b^2 V_{cb} V_{tb}^* \\ (\tilde{m}_{U_R}^2)_{23} &= \tilde{m}^2 c_1 (Y_u^\dagger Y_d Y_d^\dagger Y_u)_{23} = \tilde{m}^2 c_1 \lambda_t \lambda_c \lambda_b^2 V_{cb} V_{tb}^* \\ (a_u)_{23} &= A b_7 (Y_d Y_d^\dagger Y_u)_{23} = A b_7 \lambda_t \lambda_b^2 V_{cb} V_{tb}^* \\ (a_u)_{32} &= A b_7 (Y_d Y_d^\dagger Y_u)_{32} = A b_7 \lambda_c \lambda_b^2 V_{cb} V_{tb}^* . \end{aligned} \quad (16)$$

In writing these expressions we have neglected terms proportional to the charm Yukawa. These contributions are negligible unless the LR stop mixing

is tuned to nearly zero. With these off-diagonal soft terms, the stop-charm-neutralino couplings are

$$y_L = \frac{\lambda_b^2 V_{cb} V_{tb}^*}{m_t^2 - m_{\tilde{c}_L}^2} (\tilde{m}^2 b_2 c_{\tilde{t}} + A v_u b_7 \lambda_t s_{\tilde{t}}) \left( -\frac{g'}{3\sqrt{2}} N_{11} - \frac{g}{\sqrt{2}} N_{21} \right), \quad (17)$$

$$y_R = \mathcal{O}(\lambda_c) \quad (18)$$

where  $c_{\tilde{t}} = \cos \theta_{\tilde{t}}$  and  $s_{\tilde{t}} = \sin \theta_{\tilde{t}}$  correspond to the LR stop mixing,  $v_u$  is the up-type Higgs expectation value, and  $N_{ij}$  is the neutralino mixing matrix. Note that the relevant contributions to the FV decay width correspond to the stop mixing into the left-handed charm squark  $\tilde{c}_L$ . All the contributions involving the right-handed  $\tilde{c}_R$  squark are proportional to the charm Yukawa, which are subleading and are neglected here.

We compute the FV decay widths by calculating the mass spectrum (without flavour mixing) with SuSpect 2.41 [42]. Comparing with SoftSusy 3.3.5, corrections to the masses and the LR mixing from off-diagonal soft terms are small provided the flavour-diagonal terms match up. Using these masses, we then apply Eqs. (15,17,18) to obtain the decay width.

## 4.2 Other Decay Modes

For the 2B, 3B, and 4B modes, we use SuSpect 2.41 [42] to calculate the mass spectrum and we interface it with SUSY-HIT [88] to find the decay widths. While the 2B and 3B channels are treated in full, the SUSY-HIT implementation of the 4B mode is an approximation to the full result [22] where the outgoing  $f\bar{f}'$  fermion decay products are treated as massless. We expect this to be a good approximation except for very close to the kinematic boundary where we apply a phase space factor to account for the fermion masses.

## 4.3 Phase Diagrams

With the decay widths in hand, we can chart out the dominant decay channels in different regions of the underlying parameter space. We find that the most likely decay channels are determined largely by phase-space considerations, which depend in turn on the stop, chargino, and neutralino masses. When the 2B and 3B channels are disallowed, we also find that the 4B mode can overcome the FV mode within the MFV framework.

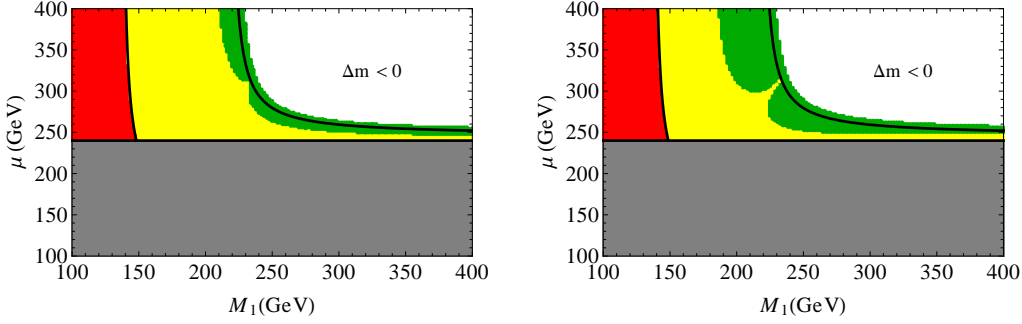


Figure 2: Dominant stop decay modes of a stop with mass  $m_{\tilde{t}} = 225$  GeV for  $\tan \beta = 10$ , with  $\cos \theta_{\tilde{t}} = 0.1$  (left) and  $\cos \theta_{\tilde{t}} = 0.7$  (right). The four regions correspond to dominant decays by the 2B (gray), 3B (red), 4B (yellow) and FV (green) channels. We also show the kinematic boundaries between these decay channels by solid black lines.

In Fig. 2 we show the dominant decay channel of the lightest stop in the  $M_1$ – $\mu$  plane for a stop mass of  $m_{\tilde{t}} = 225$  GeV,  $\tan \beta = 10$ , and mixing angles of  $\cos \theta_{\tilde{t}} = 0.1$  (left) and  $\cos \theta_{\tilde{t}} = 0.7$  (right). The four regions in the plots correspond to dominant decays by the 2B (gray), 3B (red), 4B (yellow) and FV (green) channels. The phase space boundaries between the various decay channels are shown with solid black lines. In these plots we have also fixed  $M_2 = 350$  GeV,  $M_A = 500$  GeV and  $b_2 = b_7 = 0.5$ . All other input terms are as described at the end of Sec. 2.

From these plots we see that the 2B channel dominates for smaller values of  $\mu$ , when  $m_{\tilde{t}} > m_b + m_{\chi_1^+}$  and the decay is open. This is to be expected, since the channel is neither suppressed by phase space nor flavour mixing. As this mode turns off, the 3B channel comes to dominate at smaller values of  $M_1$  where it is allowed, up to  $m_{\tilde{t}} > m_b + m_W + m_{\chi_1^0}$ . For larger  $M_1$ , the 3B channel shuts off as well and the 4B and FV channels take over. The boundaries between these regions are also nearly identical to the phase space boundaries. Note that the 4B channel is cut off when  $(m_{\tilde{t}} - m_{\chi_1^0}) < m_b$ , in which case the FV mode is all that is left.

The interplay between the 4B and FV decay modes is more complicated. While the 4B mode has significant suppression from the four-body final-state phase space, the FV channel is reduced by the level of flavour mixing. Very approximately, the relative suppression factors are  $1/4!(4\pi)^4 \sim 2 \times 10^{-6}$  for the 4B decay and  $(m_b \tan \beta/v)^4 |V_{cb}|^2 \sim 5 \times 10^{-6} (\tan \beta/10)^4$ . However, FV decays can receive further suppression if the light stop is mostly right-handed, or they can be enhanced for larger values of  $\tan \beta$ .

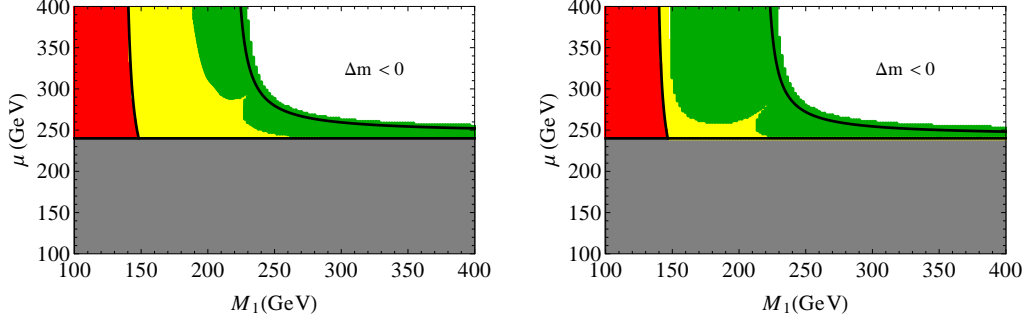


Figure 3: Dominant stop decay modes of a stop with mass  $m_{\tilde{t}} = 225$  GeV for  $\tan \beta = 30$ , with  $\cos \theta_{\tilde{t}} = 0.1$  (left) and  $\cos \theta_{\tilde{t}} = 0.7$  (right). The four regions correspond to dominant decays by the 2B (gray), 3B (red), 4B (yellow) and FV (green) channels. We also show the kinematic boundaries between these decay channels by solid black lines.

Comparing the left and right panels of Fig. 2, the enhancement of the FV channel relative to 4B with increasing  $\tilde{t}_L$  component is evident. When the lightest state is mostly right-handed, as in the left panel of the figure where  $\cos \theta_{\tilde{t}} = 0.1$ , the 4B decay dominates over the FV nearly up to the kinematic limit. For this reason, together with the mass hierarchy between the stop and the scharm, we obtain a larger branching fraction in the 4B mode relative to previous analyses [21, 89].

When the stops are maximally mixed,  $\cos \theta_{\tilde{t}} = 0.7$ , the FV channel takes over well beyond the kinematic boundary. This trend continues as the left-handed content of the light stop is increased further. However, this also gives rise to a light sbottom squark and a new decay channel  $\tilde{t} \rightarrow \tilde{b}W^{+(*)}$  that can dominate in what would otherwise be the 4B and 3B regions. Given the very strong direct-search constraints on a light sbottom as well as the indirect bounds from precision electroweak and flavour mixing, we do not consider this possibility here.

The FV mode can also be enhanced relative to the 4B mode for larger values of  $\tan \beta$ . In Fig. 3 we show the dominant stop decay channels for nearly the same parameters as in Fig. 2,  $m_{\tilde{t}} = 225$  GeV,  $M_2 = 350$  GeV,  $b_2 = b_7 = 0.5$ , but now with  $\tan \beta = 30$  (instead of  $\tan \beta = 10$ ). In the left panel we have  $\cos \theta_{\tilde{t}} = 0.1$ , and  $\cos \theta_{\tilde{t}} = 0.7$  in the right. As suggested by our simple estimates, the FV channel dominates over a significantly larger region than before. We conclude that, in MFV, either the FV or 4B decay modes can dominate in this region of the superpartner spectrum, and it is important to search for both.

The absolute decay widths obtained in the FV-4B region receive a sig-

nificant amount of suppression. Even so, we find that they are generally prompt on collider time scales unless the stop-LSP mass difference becomes very small, in agreement with Ref. [87]. For our collider studies, we will assume that all the decays are prompt. However, the emergence of a displaced stop decay vertex could allow for the direct measurement of the underlying flavour structure [87], and would be interesting to study in its own right. On the other hand, a stop that is long-lived on the time scale of the LHC detectors is firmly ruled out to masses well over  $m_{\tilde{t}_1} > 500$  GeV [90].

## 5 LHC Search Sensitivity

In this section we investigate the sensitivity of existing LHC searches to a very light stop decaying via the FV, 4B, or 3B modes. We make use of public ATLAS and CMS analyses to estimate exclusion limits in the  $m_{\tilde{t}} - m_{\chi_1^0}$  plane for stop masses in the range 100-350 GeV. Although these experimental studies were not optimized for light stops, we find that they imply quite stringent bounds on such a state.

Throughout our investigation, we treat the light stop within a simplified model where it decays exclusively (and promptly) via the FV, 4B, or 3B modes to a neutralino LSP and SM particles within the corresponding kinematically relevant region of the  $m_{\tilde{t}} - m_{\chi_1^0}$  plane. As seen in the previous section, varying the LR stop mixing,  $\tan\beta$ , or the amount of flavour mixing can modify the relative branching ratios of the FV and 4B channels.<sup>5</sup> Exclusion limits for intermediate cases can be obtained by interpolating between the separate FV and 4B cases studied here. We do not consider light sbottoms, or production via gluinos or other superpartners.

### 5.1 Event Generation and Simulation

We generate  $pp \rightarrow \tilde{t}\tilde{t}^*$  events at  $\sqrt{s} = 7$  TeV using MadGraph5 v1.4.3 [91]. The parton-level output is passed to Pythia 6.4 [92] for decays, showering, hadronization, and matching of parton showers to matrix elements. For

---

<sup>5</sup> While these decay modes are usually prompt, they are slow enough that the stop will hadronize before it decays. We do not attempt to account for this effect, but we expect that it will only be significant close to the kinematic cutoffs based on the typical momenta of the decay products.

matched samples, the MLM scheme is used with shower- $k_{\perp}$  and  $Q_{\text{match}} = 50$  GeV.

Simulation of the LHC detectors is performed with Delphes [93], using the anti- $k_T$  jet reconstruction algorithm. ATLAS and CMS detector/trigger cards are applied to obtain a more realistic comparison of our analyses to the respective LHC searches. We have cross-checked our results with PGS4 (using cone jet reconstruction with  $\Delta R=0.7$ ) [94]. The differences in the distributions of hardest jet  $p_T$  and missing energy ( $\cancel{E}_T$ ) are within generally within 5-10% for the two detector simulators. In terms of acceptances to various searches, Delphes tends to be somewhat lower than PGS.

In generating stop samples for our analysis, we are faced with a practical challenge. Many of the existing LHC SUSY searches are geared towards finding relatively heavy coloured states that decay to a much lighter LSP. These searches frequently require multiple hard jets and apply strong cuts on  $\cancel{E}_T$  or  $m_{\text{eff}} = \sum_j p_T + \cancel{E}_T$ . As such, they are typically only sensitive to the FV or 4B stop decay modes in certain specific regions of the stop-production phase space.

Since we are investigating relatively light stops, the typical energy scale in the events tends to be somewhat small. Furthermore, the momenta of the stop decay products are distributed between multiple final states in the 4B channel, and are also limited in the FV channel when the stop-LSP mass difference is small. Thus, the light stop events usually produce soft decay products and small amounts of  $\cancel{E}_T$ , particularly if the LSPs are emitted back-to-back. For these light stop events to pass many of the LHC SUSY analysis cuts, they must be produced in conjunction with one or more hard jets. In addition to increasing the total energy in the event, the radiated jet gives a net boost to the  $\tilde{t}\tilde{t}^*$  system which can lead to an observationally significant amount of missing energy [95, 96].

The challenge, therefore, is to simulate efficiently this small corner of the stop production phase space where one or more hard jets are emitted without being swamped by the much larger portion where the additional jets are relatively soft. For this, we investigated the following generator-level samples:

$$\tilde{t}\tilde{t}^*, \quad \tilde{t}\tilde{t}^* + 1j \text{ (unmatched)}, \quad \tilde{t}\tilde{t}^* + 1j \text{ (matched)},$$

with matching scale  $Q_{\text{match}} = 50$  GeV for 1j matched, and requiring  $p_T > 50, 100, 150, 200, 250, 300$  GeV for the hardest jet at the parton level in the

unmatched samples. Of these, the matched sample is expected to best reproduce the full  $p_T$  distribution of the additional jet [97]. However, each given sample is strongly dominated by events where the extra jet lies near the matching scale, leading to poor statistics in the higher- $p_T$  region of greatest interest.

To improve the statistics of the samples we generate, we compared the matched sample to a set of unmatched  $\tilde{t}\tilde{t}^* + 1j$  samples constrained to have a jet  $p_T$  greater than 50 – 300 GeV. For our comparison, we studied the relative signals predicted by these samples for a range of fiducial kinematic cuts typical of the ATLAS and CMS analyses considered in this paper:

$$\begin{array}{ll} \cancel{E}_T > 130, 200, 300 \text{ GeV} & m_{eff} > 500, 700, 1000 \text{ GeV} \\ H_T > 350, 500, 600 \text{ GeV} & p_{T,j1} > 80, 130 \text{ GeV} . \end{array}$$

We find that the  $\tilde{t}\tilde{t}^* + 1j$  unmatched sample with  $p_{T,j1} > 150$  GeV provides a good balance between obtaining useful event statistics (*i.e.* a reasonable fraction of the generated events pass the kinematic cuts) and not artificially eliminating the signals. For example, the unmatched sample with  $p_{T,j1} > 100$  GeV leads to the same effective signals to within 10–20%.

We have also compared the  $p_T$  distribution of hardest-jet in the  $1j$  unmatched sample with  $p_{T,j1} > 150$  GeV to matched samples with one or two additional hard jets. Relative to the matched  $1j$  sample with  $Q_{cut} = 50$  GeV, we find excellent agreement for  $p_{T,j1} > 150$  GeV (as is expected). Comparing to the matched  $2j$  sample (matched with  $H_T > 100$  GeV), we also get excellent agreement for the  $p_{T,j1}$  distributions. While the  $2j$  matched sample tends to produce a harder second jet, we find that including it does not appreciably increase the effective signals that pass our sample kinematic cuts.

The stop production sample we generate arises at NLO and represents only a small subset of the total stop production phase space. As a result, we do not attempt to apply a K-factor to the cross section obtained by comparing the inclusive LO and NLO cross sections (which is about 1.4 in this case based on Prospino2.1 [98]). Instead, we estimate the effect of the theory uncertainty in the cross section on the LHC exclusions by simply varying the MadGraph production cross sections by  $\pm 50\%$ .

## 5.2 LHC Searches and Exclusions

The LHC analyses that we apply to our light stop samples are summarized in Tables 1 and 2. These searches constrain different regions of the  $m_{\tilde{t}} - m_{\chi_1^0}$

ATLAS Analysis ( $\mathcal{L}/fb^{-1}$ )	Final states	Decay channel
Monojet (1.00) [99]	$\leq 1-3j, 0l$	FV, 4B
Jets+ $\cancel{E}_T$ (1.04) [44]	$\geq 2-4j, 0l$	FV, 4B
Monojet (4.7) [100]	$\leq 2j, 0l$	FV, 4B
$j + b + \cancel{E}_T$ (0.83) [101]	$\geq 3j, \geq 1b, 0l$	-
$j + l + \cancel{E}_T$ (1.04) [102]	$\geq 3-4j, 1l$	-
$j + b + l + \cancel{E}_T$ (1.03) [103]	$\geq 4j, \geq 1b, 1l$	-
$j + b + l + \cancel{E}_T$ (2.05) [104]	$\geq 3-4j \geq 1b, 0-1l$	-
$\tilde{t}\tilde{t}^* \rightarrow ll$ (4.7) [105]	$\geq 1j, 1l$	-
$j + l + b + \cancel{E}_T$ (4.7) [106]	$\geq 4j, 1b, 1l$	-
$j + b + \cancel{E}_T$ (4.7) [107]	$\geq 4j, \geq 2b, 1l$	-

Table 1: Summary of ATLAS searches at  $\sqrt{s} = 7$  TeV that constrain the FV, 4B and 3B decay modes.

plane, and taken together, provide significant bounds on a light stop. All the searches considered have  $\sqrt{s} = 7$  TeV. We defer an analysis of the recent SUSY search results obtained at  $\sqrt{s} = 8$  TeV, which appeared as this paper was nearing completion, to a future study.

We consider stop decays in the FV, 4B, and 3B modes, and the limits from each LHC analysis are applied separately. In every case, we impose the selection requirements described in the corresponding report to our simulated signal and we compare to the listed backgrounds (accounting for the stated background uncertainties) to obtain limits on the stop and neutralino masses. The corresponding 95 % c.l. exclusions are summarized in Fig. 4 (FV, 4B) and Fig. 5 (3B). In these figures, we show the result for the central value of the MadGraph-generated cross section with solid lines, and the exclusions when this cross section is varied by  $\pm 50$  % with dashed and dotted lines.

Note that many of the searches listed in Tables 1 and 2 do not yield a constraint. This fact is shown in the rightmost column of the Tables, where we list the decay channels for which the corresponding searches are relevant; when no channel is listed, no interesting bound was obtained. In the discussion to follow, we will focus on the LHC analyses that do lead to limits.

CMS Analysis ( $\mathcal{L}/fb^{-1}$ )	Final states	Decay channel
Monojet (1.1) [108]	$\leq 2j, 0l$	FV, 4B
$j + \cancel{E}_T$ (1.1) [109]	$\geq 3j, 0l$	-
$\alpha_T$ (1.14) [110]	$\geq 2j, 0-1l(\mu), 0-1\gamma$	-
$j + b + \cancel{E}_T$ (1.1) [111]	$\geq 3-4j, \geq 1b1l, \geq 1b$	FV, 4B
Razor (4.4) [112]	$\geq 2j, 0-2l$	FV, 4B, 3B
$j + l + \cancel{E}_T$ (1.1) [113]	$\geq 3-4j, 1l$	-
$M_{T2}$ (1.1) [114]	$\geq 3-4j, \geq 0-1b, 0l$	FV, 4B, 3B
Monojet (5.0) [115]	$\leq 2j, 0l$	FV, 4B
$j + \cancel{E}_T$ (4.98) [45]	$\geq 3j, 0l$	FV, 4B
$\alpha_T$ (4.98) [116]	$\geq 2j, 0-3b, 0l,$	-
$j + b + \cancel{E}_T$ (4.98) [117]	$\geq 3j, 1-3b, 0l$	FV, 4B, 3B
Razor (4.7) [118]	$\geq 2j, \geq 1b, 0-2l$	FV, 4B, 3B
$M_{T2}$ (4.73) [119]	$\geq 3-4j, \geq 0-1b, 0l$	FV, 4B, 3B

Table 2: Summary of CMS searches at  $\sqrt{s} = 7$  TeV that constrain the FV, 4B and 3B decay modes.

### 5.2.1 FV mode

The FV mode has  $\tilde{t} \rightarrow c\chi_1^0$ , which suggests that it will be probed most effectively by searches for jets and missing energy. Thus, we apply the ATLAS and CMS monojet, jets+ $\cancel{E}_T$ , Razor, and  $M_{T2}$  analyses to it. However, due to a sizable mistag rate for  $c$  jets to be identified as  $b$  jets (about 10 %), we find that the FV mode is also constrained by several  $b$ -jet analyses. In contrast, we find that searches with leptonic final states are generally not sensitive to this decay channel. The regions of the stop-neutralino mass plane excluded by the analyses we consider for the FV decay mode are shown in the left set of panels in Fig. 4.

Monojet searches require at least one hard jet and missing energy, and they are good probes of the small  $m_{\tilde{t}} - m_{\chi_1^0}$  region where the outgoing charm quark is soft and difficult to detect [23]. In this case, the hard jet arises from QCD radiation. ATLAS and CMS monojet searches apply various sets of cuts on the transverse momentum of the hardest jet  $p_{T_{j_1}}$  and the missing energy  $\cancel{E}_T$ . They also veto on events with hard leptons, as well as events with too many additional hard jets [99, 100, 108, 115]. We find that the harder cuts on  $p_{T_{j_1}}$  and  $\cancel{E}_T$  used by these analyses, which range up to 500 GeV, tend to

be the most effective at probing the stop signal. Among the set of events that pass the selection requirements, the stops must be created with a very hard extra jet. This can give the stop pair a large  $p_T$ , which leads to significant missing energy but can also make the charm jets visible. From this point of view, the less-stringent veto on additional jet activity in Refs. [100, 115] relative to Ref. [99] is beneficial.<sup>6</sup>

The presence of one or more hard QCD jets and the resulting boost of the stops can lead to multiple hard jets in FV stop events. Thus, searches for multiple jets and missing energy can also be sensitive to light stops. The recent ATLAS jets+ $\cancel{E}_T$  analysis of Ref. [44] divides their search into 2–4  $j$  channels, and imposes a lepton veto and cuts on  $\cancel{E}_T$  and  $m_{eff} = \sum_j p_{T_j} + \cancel{E}_T$ . The  $m_{eff}$  and  $\cancel{E}_T$  requirements of this analysis are geared towards heavier superpartners and are quite severe, with  $m_{eff}$  typically greater than 1000 GeV, limiting their sensitivity. In fact, the more recent ATLAS analysis of Ref. [106] with  $4.7\text{ fb}^{-1}$  of data imposes even stronger requirements on  $m_{eff}$  and is less sensitive than Ref. [44], despite having much more data. The kinematic requirements for the corresponding CMS searches for jets+ $\cancel{E}_T$  are less severe, and give slightly stronger exclusions. The CMS search for jets and missing energy of Ref. [45] requires at least 3 jets,  $H_T = \sum_j p_{T_j} > 500\text{ GeV}$ , missing energy, and no hard leptons. This search places strong limits on cross-sections for new physics, excluding a region of the  $m_{\tilde{t}} - m_{\chi_1^0}$  plane that is complementary to the monojet analyses.

The FV mode is also constrained by searches involving  $b$  jets due to the significant ( $\sim 10\%$ ) mistag rate of  $c$ -jets. The minimal requirements of the CMS jets+b+ $\cancel{E}_T$  search [111], at least three jets with  $p_T > 50\text{ GeV}$  and a  $b$  tag, can be satisfied in this case.<sup>7</sup> This analysis also has weaker cuts on  $H_T$  and missing energy (limited via the  $\alpha_T$  variable) relative to the jets+ $\cancel{E}_T$  searches, which leads to a significant exclusion of the FV mode. Let us also point out that the observation of a light squark in multiple light- and heavy-quark flavour channels could provide information about the flavour structure of the stop decay. Even though the  $c$  quark is misidentified in this case, the decay could still be differentiated from other flavour-violating channels such as  $\tilde{t} \rightarrow u\chi_1^0$ , (which is negligible in MFV), since the mistag rate of  $u$ -jets as  $b$ -jets is about 1%.

---

<sup>6</sup>The bounds from the monojet searches are also likely to be valid when the stop decay is slightly displaced.

<sup>7</sup> A small fraction (about 5%) of the stop events passing the cuts have genuine  $b$  jets produced in the parton shower.

Light stops are also constrained by the CMS Razor and  $M_{T2}$  searches. The Razor variables provide a way to use event-shape information to reduce backgrounds while not imposing overly strict kinematic requirements [112, 118]. The stop signal populates mainly the  $M_R < 1000$  GeV region, and the analysis of Ref. [112] restricts a significant part of the stop-LSP mass plane. The CMS  $M_{T2}$  analyses of Refs. [114, 119] have two separate signal regions, with and without a  $b$ -tag requirement. Applying the analysis of Ref. [114], the *High* $M_{T2}$  search channel ( $\geq 3j, 0b$ ) excludes a greater region than the *Low* $M_{T2}$  channel ( $\geq 4j, \geq 1b$ ) due to the  $b$ -tag requirement of the latter. Similar exclusions are found for the more recent search of Ref. [119]. While this analysis has considerably more data than Ref. [114], it also imposes more stringent kinematic requirements leading to about the same exclusion.

Our results for the FV mode appear to be compatible with previous analyses of this channel in the monojet and jets+ $\cancel{E}_T$  channels [25, 26, 27, 28, 37], although Ref. [34] obtains a somewhat stronger limit from the jets+ $\cancel{E}_T$  channel than we do. The limits obtained in the MT2/Razor analyses also appear to be consistent with Ref. [37], while our jets+b+ $\cancel{E}_T$  search is new and provides a slightly stronger exclusion.

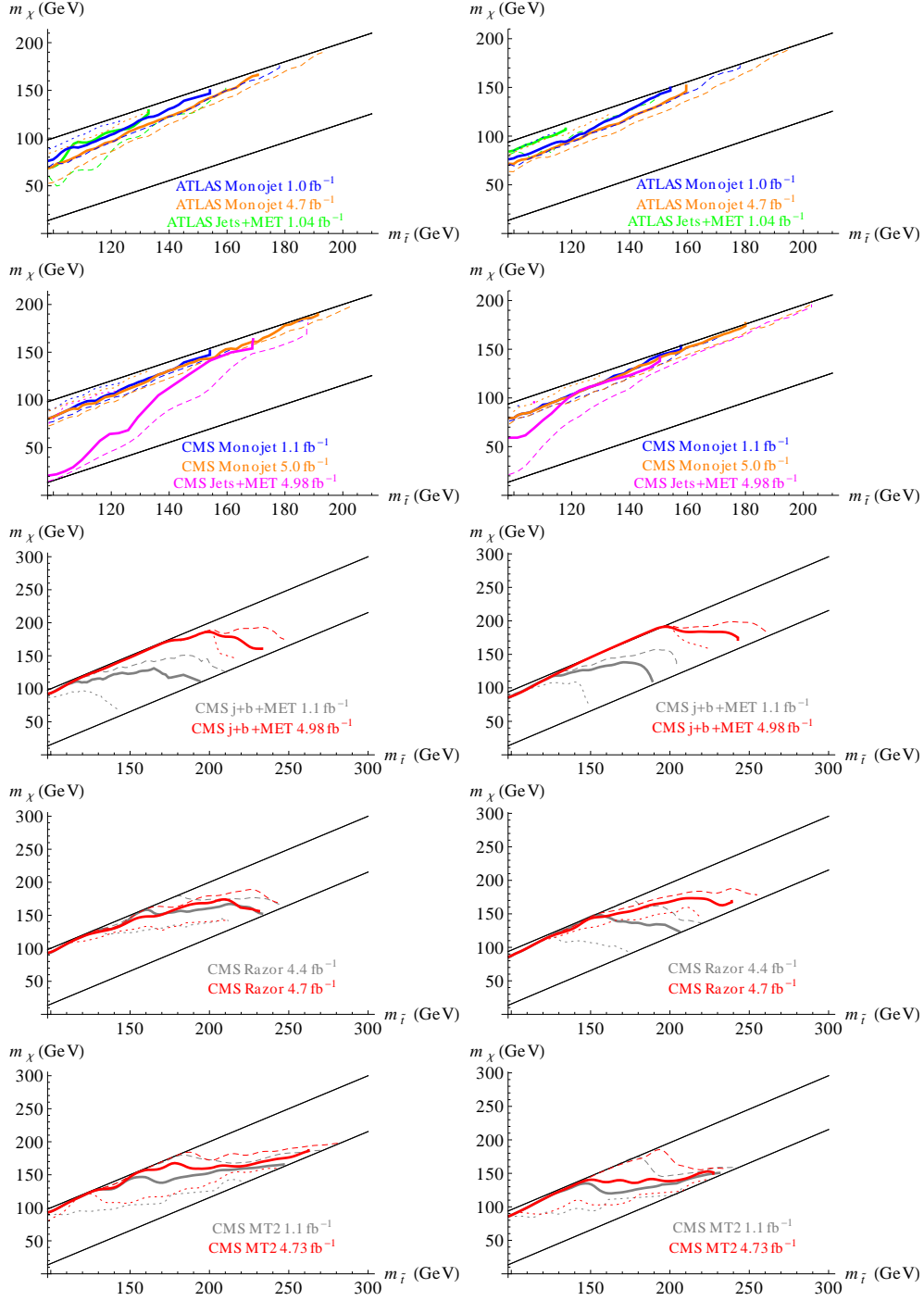


Figure 4: ATLAS and CMS exclusions on FV mode (left) and 4B mode (right). The two straight, diagonal lines correspond to  $m_{\tilde{t}} = m_{\chi_1^0}$  (upper, FV),  $m_{\tilde{t}} = m_{\chi_1^0} + m_b$  (upper, 4B), and  $m_{\tilde{t}} = m_{\chi_1^0} + m_b + m_W$  (lower, both). The dashed/dotted lines correspond to varying the cross section by  $\pm 50\%$ . The upper straight lines are the kinematic limits for these modes, while below the lower straight line we expect the 3B channel to take over.

### 5.2.2 4B mode

Each 4B stop decay produces the final state  $\tilde{t} \rightarrow b f \bar{f}' \chi_1^0$ , where the  $f \bar{f}'$  fermions come from the decay of an off-shell  $W^+$ . Events with a pair of stops can therefore produce zero, one, or two leptons. While the potential presence of leptons might seem promising, we find that they tend to be somewhat soft and difficult to identify when produced by this decay mode.<sup>8</sup> Hadronic analyses turn out to be more effective, although their reach is slightly weaker than for the FV decay channel. Let us also mention that 4B decays were performed in Pythia 6.4 [92] which uses a flat matrix element and may be a poor approximation near kinematic boundaries. We defer an attempt to implement the full decay matrix element to a future study.

Among the primarily hadronic search channels, we find that the ATLAS and CMS monojet and jets+ $\cancel{E}_T$  analyses are moderately effective. The monojet searches are sensitive mainly to the case where the hard jet is produced by QCD radiation, and as a result the 4B region excluded by the monojet searches is similar to the FV case. The ATLAS jets+ $\cancel{E}_T$  search of Ref. [44] requiring two hard jets is effective for probing the small  $(m_{\tilde{t}} - m_{\chi_1^0})$  region. However, the higher number of final states in the 4B decay results in softer jets relative to FV decays and a smaller exclusion region. We find a similar result for the CMS jets+ $\cancel{E}_T$  search of Ref. [45].

The CMS Razor analyses [112, 118] constrain the hadronic 4B mode only in the hadronic (*HAD*) channel. Although some of the Razor analyses also search for one or two  $e$  or  $\mu$  in the final state, the leptonic 4B channel is not picked up by the search. The light stop decays are constrained by the low transverse mass search region,  $M_R < 1000$  GeV, and as a result, the excluded region is similar to the FV mode. The more recent search of Ref. [118] has an additional  $b$ -tag requirement and more data, and excludes a larger region.<sup>9</sup> Similarly, the CMS  $M_{T2}$  analyses of Refs. [114, 119] that demand a  $b$ -tag are also effective. However, the net exclusions of these analyses are slightly weaker than for the FV mode, due to the higher multiplicity and softer momenta of the 4B stop decay products. Searches for  $b$ -jets and missing energy at CMS (with a lepton veto) are also effective at probing the 4B decay [111, 117].

---

<sup>8</sup>The requirement of multiple hard jets in these analyses is also problematic.

<sup>9</sup>The result of Ref. [120], that appeared after the original version of this work was submitted, suggests an even larger exclusion is possible if the  $b$ -tag requirement is relaxed.

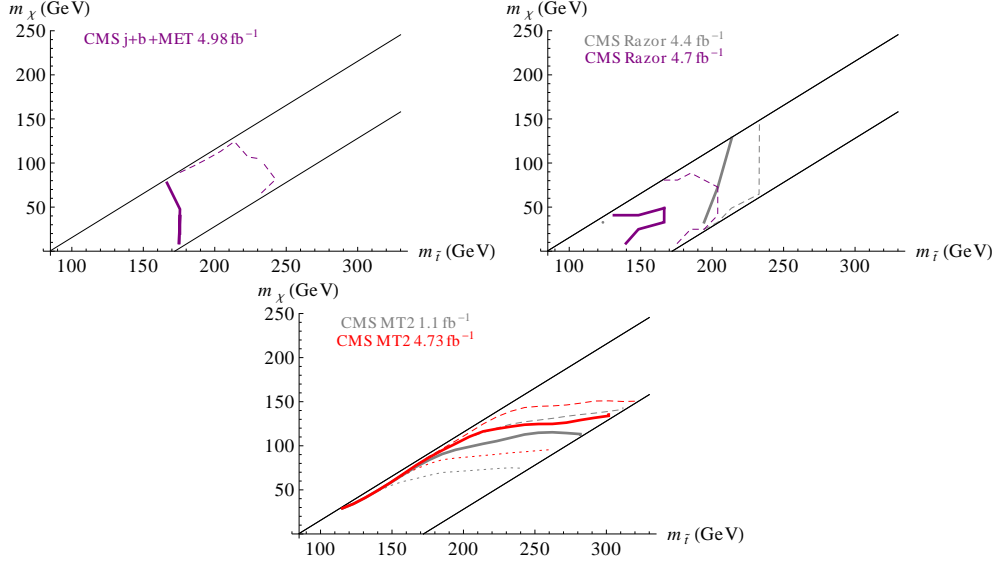


Figure 5: CMS exclusions on 3B mode. The dashed/dotted lines correspond to varying the cross section by  $\pm 50\%$ . The upper solid diagonal line shows the kinematic limit for this decay,  $m_{\tilde{t}} = m_{\chi_1^0} + m_b + m_W$ , while the lower solid diagonal line has  $m_{\tilde{t}} = m_{\chi_1^0} + m_t$  where the 2B decay channel is expected to take over.

### 5.2.3 3B mode

The 3B mode is sensitive to analyses with  $b$ -jet final states, in particular the CMS  $b$ -jet, Razor,  $M_{T2}$  analyses. The newer CMS  $b$ -jet search [117] constrains the 3B mode, with an exclusion region comparable to the FV and 4B modes. In particular, the signal region with one loose  $b$ -jet,  $1BL$ , is most sensitive to the decay mode.

The CMS Razor analyses [112, 118] are sensitive to the 3B mode in the hadronic search channel ( $HAD$ ), with stronger limits from the more recent search. The decays are constrained by the transverse mass search region,  $M_R < 1000$  GeV. The CMS  $M_{T2}$  analyses [114, 119] provide the most stringent constraints, up to  $m_{\tilde{t}} \simeq 300$  GeV. In particular, the  $b$ -tag signal region is most sensitive to the 3B decay mode.

### 5.2.4 Summary

In these analyses we have only applied existing LHC searches using up to  $5\text{ fb}^{-1}$  of data at  $\sqrt{s} = 7\text{ TeV}$ . Extending these analyses to the full  $20\text{ fb}^{-1}$  dataset at 8 TeV will improve the statistical uncertainties related to these searches by over a factor two. Since the signal-to-background ratios in most of the exclusion channels considered are typically of order unity, we expect that this to significantly improve the limits on the light stop parameter space.

Even larger improvements are likely possible in these channels with dedicated search techniques. Many of the jet and  $\cancel{E}_T$  requirements in the analyses applied here were designed for much heavier superpartners, and the resulting signal rates after cuts were often very low. The FV search could benefit from charm tagging, which would also point towards a heavy-flavour origin of the jet. In the 3B and 4B channels, additional kinematic variables such as a  $b$ -lepton invariant mass might help to isolate the signal from background and identify its origin [121].<sup>10</sup>

## 6 Conclusion

Very light stops can be consistent with current experimental bounds when they decay in ways that are challenging to detect at the LHC. In this study we have attempted to investigate the properties of light stops in a systematic way, and to estimate the bounds placed on them by indirect precision measurements and existing searches at the LHC.

When a stop is very light, it can decay according to  $\tilde{t} \rightarrow c\chi_1^0$  (FV) and  $\tilde{t} \rightarrow b f \bar{f}' \chi_1^0$  (4B). The relative branching fractions depend on the gauge content of the light stop, the value of  $\tan\beta$ , and the amount of flavour mixing within the soft parameters. When the flavour mixing is governed by MFV, it is possible for both the FV or 4B channels to be the dominant decay mode. Thus, it is important to study the signals of both possibilities at the LHC.

We have investigated the limits placed by existing LHC searches at  $\sqrt{s} = 7\text{ TeV}$  on a light stop decaying entirely in the FV, 4B, or 3B channels. Our results suggest that these searches rule out a light stop decaying in these channels unless it is heavier than at least  $m_{\tilde{t}} > 200\text{ GeV}$ . Even so, we emphasize that our results were obtained with an approximate simulation of the ATLAS and CMS detectors

---

<sup>10</sup>We thank the referee for suggesting this method.

The exclusions we obtain also imply a significant bound on electroweak baryogenesis within the MSSM. To successfully create the observed baryon asymmetry, a very light, mostly unmixed stop is required with a mass less than that of the top quark. Our results suggest that such a state is ruled out by existing LHC analyses, at least if it decays promptly in the FV, 4B, or 3B modes. Nevertheless, extensions of the MSSM that open up new decay channels might permit the stop to be as light as needed.

## Acknowledgements

We thank Wolfgang Altmanshoffer, Heather Logan, Stephen Martin, Olivier Mattelaer, Jessie Shelton, and Chiu-Tien Yu for useful conversations. Johan Alwall also provided us with invaluable help with MadGraph, Ben Allanach aided us with SoftSUSY, and Nazila Mahmoudi helped us with SuperISO. DM would also like to acknowledge the hospitality of the Perimeter Institute and the Aspen Center for Physics while this paper was under way. This research is supported by NSERC.

## A MFV Conventions and Soft Parameters

In this appendix we describe our detailed conventions for the Yukawa couplings and the soft scalar parameters under the MFV hypothesis. We also describe how to match them to those used in the SLHA2 [71] convention for specifying supersymmetric parameters.

We define the Yukawa matrices appearing in the superpotential in the same way as Ref. [87] (which follows Ref. [40]):

$$W \supset U_a^c (Y_u^\dagger)^a_i Q^i \cdot H_u - D_p^c (Y_d^\dagger)^p_i Q^i \cdot H_d , \quad (19)$$

where we have written out the explicit  $SU(3)_Q \times SU(2)_{u_R} \times SU(3)_{d_R}$  indices. The relevant soft terms in the Lagrangian are

$$\begin{aligned} -\mathcal{L}_{soft} \supset & \tilde{Q}_i^* (m_Q^2)^i_j \tilde{Q}^j + \tilde{U}_a^c (m_{U^c}^2)^a_b (\tilde{U}^{c*})^b + \tilde{D}_p^c (m_{D^c}^2)^p_q (\tilde{D}^{c*})^q \\ & + \tilde{U}_a^c (a_u^\dagger)^a_i Q^i \cdot H_u - \tilde{D}_p^c (a_d^\dagger)^p_i Q^i \cdot H_d . \end{aligned} \quad (20)$$

Both the superpotential of Eq. (19) and the soft terms of Eq. (20) are invariant under the  $G_f = SU(3)_Q \times SU(3)_{u_R} \times SU(3)_{d_R}$  flavour group with

the supermultiplets transforming as

$$Q = (3, 1, 1), \quad U^c = (1, \bar{3}, 1), \quad D^c = (1, 1, \bar{3}) , \quad (21)$$

together with the Yukawa matrices transforming according to

$$Y_u = (3, \bar{3}, 1), \quad Y_d = (3, 1, \bar{3}) . \quad (22)$$

Suppose we make a field redefinition by a  $G_f$  transformation (keeping the Yukawa matrices held fixed):

$$Q \rightarrow V_Q Q, \quad U^c \rightarrow U_u^* U^c, \quad D^c \rightarrow U_d^* D^c . \quad (23)$$

This modifies the effective Yukawa couplings appearing in Eq. (19) by

$$Y_u^\dagger \rightarrow Y_u'^\dagger = U_u^\dagger Y_u^\dagger V_Q, \quad Y_d^\dagger \rightarrow Y_d'^\dagger = U_d^\dagger Y_d^\dagger V_Q . \quad (24)$$

In this picture, the MFV hypothesis for the soft masses is equivalent to the statement that the form of the soft terms given in Eqs. (6–10) remains unchanged under such a field redefinition, provided the old Yukawa couplings are replaced by the new ones (*i.e.*  $Y_u \rightarrow Y_u'$ ,  $Y_d \rightarrow Y_d'$  in Eqs. (6–10)).

One of the two quark Yukawa matrices can be diagonalized by making  $G_f$  redefinitions. To diagonalize both simultaneously, we have to make a  $G_f$  transformation together with separate redefinitions for the two components of the  $Q = (u_L, d_L)^t$  supermultiplet,

$$u_L \rightarrow V_u u_L, \quad d_L \rightarrow V_d d_L . \quad (25)$$

This gives

$$Y_u^\dagger \rightarrow U_u^\dagger Y_u^\dagger V_u = \lambda_u \quad (26)$$

$$Y_d^\dagger \rightarrow U_d^\dagger Y_d^\dagger V_d = \lambda_d , \quad (27)$$

where  $\lambda_u = m_u/v_u$  and  $\lambda_d = m_d/v_d$  are diagonal with real, positive entries. In terms of the transformation matrices, the CKM matrix  $V$  is found to be

$$V = V_u^\dagger V_d . \quad (28)$$

This choice of field coordinates is called the super-CKM basis. Note that these combined transformations do change the form of the effective soft terms relative to the MFV forms of Eqs. (6–10).

To implement MFV soft terms, it is convenient to use  $G_f$  to choose a field basis where one of the two quark Yukawa matrices is diagonal before applying  $V_u$  and  $V_d$ . The first and most popular choice is

$$Y_d = \lambda_d, \quad Y_u = V^\dagger \lambda_u, \quad (29)$$

where  $V$  is again the CKM quark mixing matrix. This is a nice choice because we only need to transform further by  $V_u = V^\dagger$  (and  $V_d = 1$ ) to diagonalize the quark masses. We use a second, similar choice in the discussion of squarks in Section 2,

$$Y_d = V \lambda_d, \quad Y_u = \lambda_u. \quad (30)$$

The additional transformation to diagonalize the quark masses is now  $V_d = V_{CKM}$  (and  $V_u = 1$ ).

Non-diagonal scalar soft terms can be accommodated in the SLHA2 convention [71]. the down-type squark mass matrix in the super-CKM basis is

$$\mathcal{M}_d^2 = \begin{pmatrix} \hat{m}_Q^2 + m_d^2 + D_{dL} & v_d \hat{T}_d^\dagger - \mu m_d \tan \beta \\ v_d \hat{T}_d - \mu^* m_d \tan \beta & m_{\bar{D}}^2 + m_d^2 + D_{dR} \end{pmatrix}, \quad (31)$$

while the up-type squark matrix is

$$\mathcal{M}_u^2 = \begin{pmatrix} V \hat{m}_Q^2 V^\dagger + m_u^2 + D_{uL} & v_u \hat{T}_u^\dagger - \mu m_u \cot \beta \\ v_u \hat{T}_u - \mu^* m_u \cot \beta & m_{\bar{U}}^2 + m_u^2 + D_{uR} \end{pmatrix}. \quad (32)$$

Working in a  $G_f$  basis where either  $Y_u$  or  $Y_d$  is diagonal, these entries are related to the MFV soft masses using our conventions by

$$\hat{m}_Q^2 = V_d^\dagger m_Q^2 V_d = \tilde{m}^2 (a_1 \mathbb{I} + b_1 V^\dagger \lambda_u^2 V + b_2 \lambda_d^2 + \dots) \quad (33)$$

$$\hat{m}_{\bar{U}}^2 = m_{U^c}^2 = \tilde{m}^2 (a_2 \mathbb{I} + b_5 \lambda_u^2 + c_1 \lambda_u V \lambda_d^2 V \lambda_u) \quad (34)$$

$$\hat{m}_{\bar{D}}^2 = m_{D^c}^2 = \tilde{m}^2 (a_3 \mathbb{I} + b_6 \lambda_d^2) \quad (35)$$

$$\hat{T}_u = a_u^\dagger V_u = A \lambda_u (a_4 \mathbb{I} + b_7 V \lambda_d^2 V^\dagger) \quad (36)$$

$$\hat{T}_d = a_d^\dagger V_d = A \lambda_d (a_5 \mathbb{I} + b_8 V \lambda_u^2 V^\dagger). \quad (37)$$

These expressions apply for either  $Y_u$  or  $Y_d$  diagonal.

## References

- [1] S. P. Martin, *A Supersymmetry primer*, [hep-ph/9709356](#).
- [2] S. Dimopoulos and G. Giudice, *Naturalness constraints in supersymmetric theories with nonuniversal soft terms*, *Phys.Lett.* **B357** (1995) 573–578, [[hep-ph/9507282](#)].
- [3] M. Carena, G. Nardini, M. Quiros, and C. Wagner, *The Baryogenesis Window in the MSSM*, *Nucl.Phys.* **B812** (2009) 243–263, [[arXiv:0809.3760](#)].
- [4] M. Laine, G. Nardini, and K. Rummukainen, *Lattice study of an electroweak phase transition at  $m_h \sim 126$  GeV*, [arXiv:1211.7344](#).
- [5] D. E. Morrissey and M. J. Ramsey-Musolf, *Electroweak baryogenesis*, *New J.Phys.* **14** (2012) 125003, [[arXiv:1206.2942](#)].
- [6] C. Boehm, A. Djouadi, and M. Drees, *Light scalar top quarks and supersymmetric dark matter*, *Phys.Rev.* **D62** (2000) 035012, [[hep-ph/9911496](#)].
- [7] J. R. Ellis, K. A. Olive, and Y. Santoso, *Calculations of neutralino stop coannihilation in the CMSSM*, *Astropart.Phys.* **18** (2003) 395–432, [[hep-ph/0112113](#)].
- [8] C. Balazs, M. S. Carena, and C. Wagner, *Dark matter, light stops and electroweak baryogenesis*, *Phys.Rev.* **D70** (2004) 015007, [[hep-ph/0403224](#)].
- [9] C. Balazs, M. S. Carena, A. Menon, D. Morrissey, and C. Wagner, *The Supersymmetric origin of matter*, *Phys.Rev.* **D71** (2005) 075002, [[hep-ph/0412264](#)].
- [10] Y. Kats and D. Shih, *Light Stop NLSPs at the Tevatron and LHC*, *JHEP* **1108** (2011) 049, [[arXiv:1106.0030](#)].
- [11] M. Papucci, J. T. Ruderman, and A. Weiler, *Natural SUSY Endures*, *JHEP* **1209** (2012) 035, [[arXiv:1110.6926](#)].

- [12] R. Essig, E. Izaguirre, J. Kaplan, and J. G. Wacker, *Heavy Flavor Simplified Models at the LHC*, *JHEP* **1201** (2012) 074, [[arXiv:1110.6443](#)].
- [13] T. Plehn, M. Spannowsky, and M. Takeuchi, *Stop searches in 2012*, *JHEP* **1208** (2012) 091, [[arXiv:1205.2696](#)].
- [14] D. S. Alves, M. R. Buckley, P. J. Fox, J. D. Lykken, and C.-T. Yu, *Stops and MET: The Shape of Things to Come*, [arXiv:1205.5805](#).
- [15] Z. Han, A. Katz, D. Krohn, and M. Reece, *(Light) Stop Signs*, *JHEP* **1208** (2012) 083, [[arXiv:1205.5808](#)].
- [16] D. E. Kaplan, K. Rehermann, and D. Stolarski, *Searching for Direct Stop Production in Hadronic Top Data at the LHC*, *JHEP* **1207** (2012) 119, [[arXiv:1205.5816](#)].
- [17] J. Cao, C. Han, L. Wu, J. M. Yang, and Y. Zhang, *Probing Natural SUSY from Stop Pair Production at the LHC*, *JHEP* **1211** (2012) 039, [[arXiv:1206.3865](#)].
- [18] B. Dutta, T. Kamon, N. Koley, K. Sinha, and K. Wang, *Searching for Top Squarks at the LHC in Fully Hadronic Final State*, *Phys.Rev.* **D86** (2012) 075004, [[arXiv:1207.1873](#)].
- [19] C. Kilic and B. Tweedie, *Cornering Light Stops with Dileptonic  $mT_2$* , [arXiv:1211.6106](#).
- [20] I. I. Bigi and S. Rudaz, *SEARCH FOR SCALAR SUPERPARTNERS OF THE TOP QUARK*, *Phys.Lett.* **B153** (1985) 335–340.
- [21] K.-i. Hikasa and M. Kobayashi, *Light Scalar Top at  $e^+ e^-$  Colliders*, *Phys.Rev.* **D36** (1987) 724.
- [22] C. Boehm, A. Djouadi, and Y. Mambrini, *Decays of the lightest top squark*, *Phys.Rev.* **D61** (2000) 095006, [[hep-ph/9907428](#)].
- [23] M. Carena, A. Freitas, and C. Wagner, *Light Stop Searches at the LHC in Events with One Hard Photon or Jet and Missing Energy*, *JHEP* **0810** (2008) 109, [[arXiv:0808.2298](#)].

- [24] R. Demina, J. D. Lykken, K. T. Matchev, and A. Nomerotski, *Stop and sbottom searches in Run II of the Fermilab Tevatron*, *Phys.Rev.* **D62** (2000) 035011, [[hep-ph/9910275](#)].
- [25] X.-J. Bi, Q.-S. Yan, and P.-F. Yin, *Probing Light Stop Pairs at the LHC*, *Phys.Rev.* **D85** (2012) 035005, [[arXiv:1111.2250](#)].
- [26] M. A. Ajaib, T. Li, and Q. Shafi, *Stop-Neutralino Coannihilation in the Light of LHC*, *Phys.Rev.* **D85** (2012) 055021, [[arXiv:1111.4467](#)].
- [27] B. He, T. Li, and Q. Shafi, *Impact of LHC Searches on NLSP Top Squark and Gluino Mass*, *JHEP* **1205** (2012) 148, [[arXiv:1112.4461](#)].
- [28] Z.-H. Yu, X.-J. Bi, Q.-S. Yan, and P.-F. Yin, *Detecting light stop pairs in coannihilation scenarios at the LHC*, [arXiv:1211.2997](#).
- [29] M. Drees, M. Hanussek, and J. S. Kim, *Light Stop Searches at the LHC with Monojet Events*, *Phys.Rev.* **D86** (2012) 035024, [[arXiv:1201.5714](#)].
- [30] S. Kraml and A. Raklev, *Same-sign top quarks as signature of light stops at the LHC*, *Phys.Rev.* **D73** (2006) 075002, [[hep-ph/0512284](#)].
- [31] S. Bornhauser, M. Drees, S. Grab, and J. Kim, *Light Stop Searches at the LHC in Events with two b-Jets and Missing Energy*, *Phys.Rev.* **D83** (2011) 035008, [[arXiv:1011.5508](#)].
- [32] S. P. Martin, *Exploring compressed supersymmetry with same-sign top quarks at the Large Hadron Collider*, *Phys.Rev.* **D78** (2008) 055019, [[arXiv:0807.2820](#)].
- [33] S. P. Das, A. Datta, and M. Guchait, *Four-body decay of the stop squark at the upgraded Tevatron*, *Phys.Rev.* **D65** (2002) 095006, [[hep-ph/0112182](#)].
- [34] A. Choudhury and A. Datta, *New limits on top squark NLSP from LHC  $4.7\text{ fb}^{-1}$  data*, *Mod.Phys.Lett.* **A27** (2012) 1250188, [[arXiv:1207.1846](#)].
- [35] K. Ghosh, K. Huitu, J. Laamanen, L. Leinonen, K. Huitu, *et. al.*, *Top jets as a probe of degenerate stop-NLSP LSP scenario in the framework of cMSSM*, [arXiv:1207.2429](#).

- [36] G. Belanger, M. Heikinheimo, and V. Sanz, *Model-Independent Bounds on Squarks from Monophoton Searches*, *JHEP* **1208** (2012) 151, [[arXiv:1205.1463](#)].
- [37] H. Dreiner, M. Kramer, and J. Tattersall, *Exploring QCD uncertainties when setting limits on compressed SUSY spectra*, [arXiv:1211.4981](#).
- [38] W. Altmannshofer, A. J. Buras, S. Gori, P. Paradisi, and D. M. Straub, *Anatomy and Phenomenology of FCNC and CPV Effects in SUSY Theories*, *Nucl.Phys.* **B830** (2010) 17–94, [[arXiv:0909.1333](#)].
- [39] T. Hurth and F. Mahmoudi, *The Minimal Flavour Violation benchmark in view of the latest LHCb data*, *Nucl.Phys.* **B865** (2012) 461–485, [[arXiv:1207.0688](#)].
- [40] G. D’Ambrosio, G. Giudice, G. Isidori, and A. Strumia, *Minimal flavor violation: An Effective field theory approach*, *Nucl.Phys.* **B645** (2002) 155–187, [[hep-ph/0207036](#)].
- [41] G. Colangelo, E. Nikolidakis, and C. Smith, *Supersymmetric models with minimal flavour violation and their running*, *Eur.Phys.J.* **C59** (2009) 75–98, [[arXiv:0807.0801](#)].
- [42] A. Djouadi, J.-L. Kneur, and G. Moultaka, *SuSpect: A Fortran code for the supersymmetric and Higgs particle spectrum in the MSSM*, *Comput.Phys.Comm.* **176** (2007) 426–455, [[hep-ph/0211331](#)].
- [43] B. Allanach, *SOFTSUSY: a program for calculating supersymmetric spectra*, *Comput.Phys.Comm.* **143** (2002) 305–331, [[hep-ph/0104145](#)].
- [44] **ATLAS** Collaboration, G. Aad *et. al.*, *Search for squarks and gluinos with the ATLAS detector in final states with jets and missing transverse momentum using  $4.7\text{fb}^{-1}$  of  $\sqrt{s} = 7\text{ TeV}$  proton-proton collision data*, [arXiv:1208.0949](#).
- [45] **CMS** Collaboration, S. Chatrchyan *et. al.*, *Search for new physics in the multijet and missing transverse momentum final state in proton-proton collisions at  $\sqrt{s} = 7\text{ TeV}$* , *Phys.Rev.Lett.* **109** (2012) 171803, [[arXiv:1207.1898](#)].

- [46] **ATLAS** Collaboration, ATLAS-CONF-2011-166, “Search for direct top squark pair production in final states with one isolated lepton, jets, and missing transverse momentum in  $\sqrt{s} = 8$  TeV pp collisions using 13.0 fb of atlas data.”.
- [47] **ATLAS** Collaboration, ATLAS-CONF-2011-167, “Search for a supersymmetric top-quark partner in final states with two leptons in  $\sqrt{s} = 8$  TeV pp collisions using 13 fb of atlas data.”.
- [48] **ATLAS** Collaboration, ATLAS-CONF-2011-165, “Search for direct sbottom production in event with two b-jets using 12.8 fb-1 of pp collisions at  $\sqrt{s} = 8$  TeV with the atlas detector.”.
- [49] **ATLAS** Collaboration, ATLAS-CONF-2011-145, “Search for gluino pair production in final states with missing transverse momentum and at least three b-jets using 12.8 fb-1 of pp collisions at  $\sqrt{s} = 8$  TeV with the atlas detector.”.
- [50] **CMS** Collaboration, CMS-PAS-SUS-12-028, “Search for supersymmetry in final states with missing transverse energy and 0, 1, 2, 3, or at least 4 b-quark jets in 8 tev pp collisions using the variable  $\alpha_{\text{phat}}$ .”.
- [51] **OPAL** Collaboration, G. Abbiendi *et. al.*, *Search for scalar top and scalar bottom quarks at LEP*, *Phys.Lett.* **B545** (2002) 272–284, [hep-ex/0209026].
- [52] **CDF** Collaboration, T. Aaltonen *et. al.*, *Search for Scalar Top Quark Production in  $p\bar{p}$  Collisions at  $\sqrt{s} = 1.96$  TeV*, *JHEP* **1210** (2012) 158, [arXiv:1203.4171].
- [53] **D0** Collaboration, V. Abazov *et. al.*, *Search for scalar top quarks in the acoplanar charm jets and missing transverse energy final state in  $p\bar{p}$  collisions at  $\sqrt{s} = 1.96$ -TeV*, *Phys.Lett.* **B665** (2008) 1–8, [arXiv:0803.2263].
- [54] M. E. Peskin and T. Takeuchi, *Estimation of oblique electroweak corrections*, *Phys.Rev.* **D46** (1992) 381–409.
- [55] H. M. Lee, V. Sanz, and M. Trott, *Hitting sbottom in natural SUSY*, *JHEP* **1205** (2012) 139, [arXiv:1204.0802].

- [56] V. Barger, P. Huang, M. Ishida, and W.-Y. Keung, *Scalar-Top Masses from SUSY Loops with 125 GeV mh and Precise Mw*, [arXiv:1206.1777](#).
- [57] J. R. Espinosa, C. Grojean, V. Sanz, and M. Trott, *NSUSY fits*, [arXiv:1207.7355](#).
- [58] **CDF, D0** Collaboration, T. E. W. Group, *2012 Update of the Combination of CDF and D0 Results for the Mass of the W Boson*, [arXiv:1204.0042](#).
- [59] **ATLAS Collaboration** Collaboration, G. Aad *et. al.*, *Observation of a new particle in the search for the Standard Model Higgs boson with the ATLAS detector at the LHC*, *Phys.Lett.* **B716** (2012) 1–29, [[arXiv:1207.7214](#)].
- [60] **CMS Collaboration** Collaboration, S. Chatrchyan *et. al.*, *Observation of a new boson at a mass of 125 GeV with the CMS experiment at the LHC*, *Phys.Lett.* **B716** (2012) 30–61, [[arXiv:1207.7235](#)].
- [61] S. Heinemeyer, W. Hollik, and G. Weiglein, *Electroweak precision observables in the minimal supersymmetric standard model*, *Phys.Rept.* **425** (2006) 265–368, [[hep-ph/0412214](#)].
- [62] S. Heinemeyer, W. Hollik, A. Weber, and G. Weiglein, *Z Pole Observables in the MSSM*, *JHEP* **0804** (2008) 039, [[arXiv:0710.2972](#)].
- [63] G.-C. Cho, K. Hagiwara, Y. Matsumoto, and D. Nomura, *The MSSM confronts the precision electroweak data and the muon g-2*, *JHEP* **1111** (2011) 068, [[arXiv:1104.1769](#)].
- [64] R. Barbieri and G. Giudice,  *$b \rightarrow s$  gamma decay and supersymmetry*, *Phys.Lett.* **B309** (1993) 86–90, [[hep-ph/9303270](#)].
- [65] Y. Okada, *Light stop and the  $b \rightarrow s$  gamma process*, *Phys.Lett.* **B315** (1993) 119–123, [[hep-ph/9307249](#)].
- [66] G. Degrandi, P. Gambino, and G. Giudice,  *$B \rightarrow X(s$  gamma) in supersymmetry: Large contributions beyond the leading order*, *JHEP* **0012** (2000) 009, [[hep-ph/0009337](#)].

- [67] **Heavy Flavor Averaging Group** Collaboration, Y. Amhis *et. al.*, *Averages of  $b$ -hadron,  $c$ -hadron, and tau-lepton properties as of early 2012*, [arXiv:1207.1158](#).
- [68] B. Grzadkowski and M. Misiak, *Anomalous  $Wtb$  coupling effects in the weak radiative  $B$ -meson decay*, *Phys.Rev.* **D78** (2008) 077501, [[arXiv:0802.1413](#)].
- [69] **LHCb Collaboration** Collaboration, R. Aaij *et. al.*, *Strong constraints on the rare decays  $B_s \rightarrow \mu^+ \mu^-$  and  $B^0 \rightarrow \mu^+ \mu^-$* , *Phys.Rev.Lett.* **108** (2012) 231801, [[arXiv:1203.4493](#)].
- [70] F. Mahmoudi, *SuperIso v2.3: A Program for calculating flavor physics observables in Supersymmetry*, *Comput.Phys.Commun.* **180** (2009) 1579–1613, [[arXiv:0808.3144](#)].
- [71] B. Allanach, C. Balazs, G. Belanger, M. Bernhardt, F. Boudjema, *et. al.*, *SUSY Les Houches Accord 2*, *Comput.Phys.Commun.* **180** (2009) 8–25, [[arXiv:0801.0045](#)].
- [72] L. J. Hall, D. Pinner, and J. T. Ruderman, *A Natural SUSY Higgs Near 126 GeV*, *JHEP* **1204** (2012) 131, [[arXiv:1112.2703](#)].
- [73] P. Draper, P. Meade, M. Reece, and D. Shih, *Implications of a 125 GeV Higgs for the MSSM and Low-Scale SUSY Breaking*, *Phys.Rev.* **D85** (2012) 095007, [[arXiv:1112.3068](#)].
- [74] M. Carena, G. Nardini, M. Quiros, and C. E. Wagner, *MSSM Electroweak Baryogenesis and LHC Data*, [arXiv:1207.6330](#).
- [75] S. Dawson, A. Djouadi, and M. Spira, *QCD corrections to SUSY Higgs production: The Role of squark loops*, *Phys.Rev.Lett.* **77** (1996) 16–19, [[hep-ph/9603423](#)].
- [76] A. Menon and D. E. Morrissey, *Higgs Boson Signatures of MSSM Electroweak Baryogenesis*, *Phys.Rev.* **D79** (2009) 115020, [[arXiv:0903.3038](#)].
- [77] T. Cohen, D. E. Morrissey, and A. Pierce, *Electroweak Baryogenesis and Higgs Signatures*, *Phys.Rev.* **D86** (2012) 013009, [[arXiv:1203.2924](#)].

- [78] D. Curtin, P. Jaiswal, and P. Meade, *Excluding Electroweak Baryogenesis in the MSSM*, *JHEP* **1208** (2012) 005, [[arXiv:1203.2932](#)].
- [79] R. Dermisek and I. Low, *Probing the Stop Sector and the Sanity of the MSSM with the Higgs Boson at the LHC*, *Phys.Rev.* **D77** (2008) 035012, [[hep-ph/0701235](#)].
- [80] M. Carena, S. Gori, N. R. Shah, C. E. Wagner, and L.-T. Wang, *Light Stau Phenomenology and the Higgs  $\gamma\gamma$  Rate*, *JHEP* **1207** (2012) 175, [[arXiv:1205.5842](#)].
- [81] U. Ellwanger, *A Higgs boson near 125 GeV with enhanced di-photon signal in the NMSSM*, *JHEP* **1203** (2012) 044, [[arXiv:1112.3548](#)].
- [82] B. Batell, S. Gori, and L.-T. Wang, *Exploring the Higgs Portal with 10/fb at the LHC*, *JHEP* **1206** (2012) 172, [[arXiv:1112.5180](#)].
- [83] M. Drees and M. M. Nojiri, *Production and decay of scalar stoponium bound states*, *Phys.Rev.* **D49** (1994) 4595–4616, [[hep-ph/9312213](#)].
- [84] S. P. Martin, *Diphoton decays of stoponium at the Large Hadron Collider*, *Phys.Rev.* **D77** (2008) 075002, [[arXiv:0801.0237](#)].
- [85] V. Barger, M. Ishida, and W.-Y. Keung, *Searching for Stoponium along with the Higgs boson*, *Phys.Rev.Lett.* **108** (2012) 081804, [[arXiv:1110.2147](#)].
- [86] Y. Kats and M. J. Strassler, *Probing Colored Particles with Photons, Leptons, and Jets*, *JHEP* **1211** (2012) 097, [[arXiv:1204.1119](#)].
- [87] G. Hiller and Y. Nir, *Measuring Flavor Mixing with Minimal Flavor Violation at the LHC*, *JHEP* **0803** (2008) 046, [[arXiv:0802.0916](#)].
- [88] A. Djouadi, M. Muhlleitner, and M. Spira, *Decays of supersymmetric particles: The Program SUSY-HIT (SUspect-SdecaY-Hdecay-InTerface)*, *Acta Phys.Polon.* **B38** (2007) 635–644, [[hep-ph/0609292](#)].
- [89] M. Muhlleitner and E. Poppo, *Light Stop Decay in the MSSM with Minimal Flavour Violation*, *JHEP* **1104** (2011) 095, [[arXiv:1102.5712](#)].

- [90] **CMS Collaboration** Collaboration, S. Chatrchyan *et. al.*, *Search for heavy long-lived charged particles in pp collisions at  $\sqrt{s} = 7$  TeV*, *Phys.Lett.* **B713** (2012) 408–433, [[arXiv:1205.0272](#)].
- [91] J. Alwall, M. Herquet, F. Maltoni, O. Mattelaer, and T. Stelzer, *MadGraph 5 : Going Beyond*, *JHEP* **1106** (2011) 128, [[arXiv:1106.0522](#)].
- [92] T. Sjostrand, S. Mrenna, and P. Z. Skands, *PYTHIA 6.4 Physics and Manual*, *JHEP* **0605** (2006) 026, [[hep-ph/0603175](#)].
- [93] S. Ovin, X. Rouby, and V. Lemaitre, *DELPHES, a framework for fast simulation of a generic collider experiment*, [arXiv:0903.2225](#).
- [94] J. Conway, *PGS4: Pretty Good Simulator*, .
- [95] J. Alwall, M.-P. Le, M. Lisanti, and J. G. Wacker, *Searching for Directly Decaying Gluinos at the Tevatron*, *Phys.Lett.* **B666** (2008) 34–37, [[arXiv:0803.0019](#)].
- [96] J. Alwall, M.-P. Le, M. Lisanti, and J. G. Wacker, *Model-Independent Jets plus Missing Energy Searches*, *Phys.Rev.* **D79** (2009) 015005, [[arXiv:0809.3264](#)].
- [97] J. Alwall, S. de Visscher, and F. Maltoni, *QCD radiation in the production of heavy colored particles at the LHC*, *JHEP* **0902** (2009) 017, [[arXiv:0810.5350](#)].
- [98] W. Beenakker, R. Hopker, and M. Spira, *PROSPINO: A Program for the production of supersymmetric particles in next-to-leading order QCD*, [hep-ph/9611232](#).
- [99] **ATLAS Collaboration**, ATLAS-CONF-2011-096, “Search for new phenomena in monojet plus missing transverse momentum final states using  $1 \text{ fb}^{-1}$  of  $pp$  collisions at  $\sqrt{s} = 7$  TeV with the atlas detector.”.
- [100] **ATLAS Collaboration**, ATLAS-CONF-2012-084, “Search for dark matter candidates and large extra dimensions in events with a jet and missing transverse momentum with the atlas detector.”.

- [101] **ATLAS** Collaboration, ATLAS-CONF-2011-098, “Search for supersymmetry in pp collisions at  $\sqrt{s} = 7$  tev in final states with missing transverse momentum, b-jets and no leptons.”.
- [102] **ATLAS** Collaboration, G. Aad *et. al.*, *Search for supersymmetry in final states with jets, missing transverse momentum and one isolated lepton in  $\sqrt{s} = 7$  TeV pp collisions using  $1 \text{ fb}^{-1}$  of ATLAS data*, *Phys.Rev.* **D85** (2012) 012006, [[arXiv:1109.6606](#)].
- [103] **ATLAS** Collaboration, ATLAS-CONF-2011-130, “Search for supersymmetry in pp collisions at  $\sqrt{s}=7$  tev in final states with missing transverse momentum, b-jets and one lepton with the atlas detector.”.
- [104] **ATLAS** Collaboration, G. Aad *et. al.*, *Search for supersymmetry in pp collisions at  $\sqrt{s} = 7$  TeV in final states with missing transverse momentum and b-jets with the ATLAS detector*, *Phys.Rev.* **D85** (2012) 112006, [[arXiv:1203.6193](#)].
- [105] **ATLAS** Collaboration, ATLAS-CONF-2012-059, “Search for light scalar top quark pair production in final states with two leptons with the atlas detector in  $\sqrt{s}=7$  tev proton–proton collisions.”.
- [106] **ATLAS** Collaboration, ATLAS-CONF-2012-073, “Search for direct top squark pair production in final states with one isolated lepton, jets, and missing transverse momentum in  $\sqrt{s} = 7$  tev pp collisions using  $4.7 \text{ fb}^{-1}$  of atlas data.”.
- [107] **ATLAS** Collaboration, ATLAS-CONF-2012-070, “Search for light scalar top pair production in final states with leptons and b-jets with the atlas detector in  $\sqrt{s} = 7$  tev proton-proton collisions.”.
- [108] **CMS** Collaboration, CMS-PAS-EXO-11-059, “Search for dark matter and large extra dimensions in monojet events in pp collisions at  $\sqrt{s}=7$  tev.”.
- [109] **CMS** Collaboration, CMS-PAS-SUS-11-004, “Search for supersymmetry in all-hadronic events with missing energy.”.

- [110] **CMS** Collaboration, S. Chatrchyan *et. al.*, *Search for Supersymmetry at the LHC in Events with Jets and Missing Transverse Energy*, *Phys.Rev.Lett.* **107** (2011) 221804, [[arXiv:1109.2352](#)].
- [111] **CMS** Collaboration, CMS-PAS-SUS-11-006, “Search for new physics in events with b-quark jets and missing transverse energy in proton-proton collisions at 7 tev.”.
- [112] **CMS** Collaboration, CMS-PAS-SUS-12-005, “Search for supersymmetry with the razor variables at  $s = 7$  tev.”.
- [113] **CMS** Collaboration, CMS-PAS-SUS-11-015, “Search for supersymmetry in events with a lepton and missing energy.”.
- [114] **CMS** Collaboration, CMS-PAS-SUS-11-005, “Search for supersymmetry in all-hadronic events with  $mt_2$ .”.
- [115] **CMS** Collaboration, S. Chatrchyan *et. al.*, *Search for dark matter and large extra dimensions in monojet events in pp collisions at  $\sqrt{s}=7$  TeV*, [arXiv:1206.5663](#).
- [116] **CMS** Collaboration, CMS-PAS-SUS-11-022, “Search for supersymmetry in final states with missing transverse energy and 0, 1, 2, or 3 b jets in 7 tev pp collisions.”.
- [117] **CMS** Collaboration, CMS-PAS-SUS-12-003, “Search for supersymmetry in events with b-quark jets and missing transverse energy in pp collisions at 7 tev.”.
- [118] **CMS** Collaboration, CMS-PAS-SUS-11-024, “Search for supersymmetry in final states with b-jets using the razor variables at  $s = 7$  tev.”.
- [119] **CMS** Collaboration, S. Chatrchyan *et. al.*, *Search for supersymmetry in hadronic final states using  $MT_2$  in pp collisions at  $\sqrt{s} = 7$  TeV*, *JHEP* **1210** (2012) 018, [[arXiv:1207.1798](#)].
- [120] A. Delgado, G. F. Giudice, G. Isidori, M. Pierini, and A. Strumia, *The light stop window*, *Eur.Phys.J.* **C73** (2013) 2370, [[arXiv:1212.6847](#)].

- [121] C.-L. Chou and M. E. Peskin, *Scalar top quark as the next-to-lightest supersymmetric particle*, *Phys.Rev.* **D61** (2000) 055004, [[hep-ph/9909536](#)].